

# Modeling and Control of 5-DoF Boom Crane

Michele Ambrosino<sup>a</sup>, Marc Berneman<sup>b</sup>, Gianluca Carbone<sup>a</sup>,  
Rémi Crépin<sup>a</sup>, Arnaud Dawans<sup>c</sup>, and Emanuele Garone<sup>a</sup>

<sup>a</sup>Service d'Automatique et d'Analyse des Systèmes, Université Libre de Bruxelles, Brussels, Belgium

<sup>b</sup>Vrije Universiteit Brussel, <sup>c</sup>Entreprises Jacques Delens S.A., Brussels, Belgium

Michele.Ambrosino@ulb.ac.be, marc.berneman@vub.be, Gianluca.Carbone@ulb.ac.be,

Remi.Crepin@ulb.ac.be, adawans@jacquesdelens.be, egarone@ulb.ac.be

## Abstract -

Automation of cranes can have a direct impact on the productivity of construction projects. In this paper, we focus on the control of one of the most used cranes, the boom crane. Tower cranes and overhead cranes have been widely studied in the literature, whereas the control of boom cranes has been investigated only by a few works. Typically, these works make use of simple models making use of a large number of simplifying assumptions (e.g. fixed length cable, assuming certain dynamics are uncoupled, etc.) A first result of this paper is to present a fairly complete nonlinear dynamic model of a boom crane taking into account all coupling dynamics and where the only simplifying assumption is that the cable is considered as rigid. The boom crane involves pitching and rotational movements, which generate complicated centrifugal forces, and consequently, equations of motion highly nonlinear. On the basis of this model, a control law has been developed able to perform position control of the crane while actively damping the oscillations of the load. The effectiveness of the approach has been tested in simulation with realistic physical parameters and tested in the presence of wind disturbances.

## Keywords -

Boom cranes; Robotics; Motion control; Underactuated systems; Nonlinear control.

## 1 Introduction

A crane is a type of machine, generally equipped with a hoist rope, that is used to move materials. Cranes can be classified in overhead cranes [1]-[2], offshore cranes [3]-[4], and rotary cranes [5]-[6]. Currently, the automation of cranes is still in a relatively early phase. To improve the efficiency and safety of cranes some control approaches have been proposed using sliding-mode control [7]-[8], optimal control [9], adaptive control [10], prediction control [11], intelligent control [12].

In this paper we focus on the modeling and control of a very common type of rotary crane, known as 'boom crane'.

Compared with other cranes, boom cranes have higher flexibility and lower energy consumption. Therefore, boom cranes have been widely used in the maintenance of buildings and to handle masonry in urban streets and construction sites. There the cranes have a boom that can rotate in two directions (e.g. pitch and yaw motions) and the load swing can be split into two dimensions. Consequently, the nonlinear dynamic models of boom cranes are more complex than those of other types of cranes.

In recent years, a number of studies have been carried out to solve the control problems of such complex systems. [13]-[14] proposed the use of S-curve trajectories as an open-loop control approach to achieve anti-sway control for the payload. Moreover, input shaping has been widely applied to control boom cranes [15]. However, the open-loop control strategies are sensitive to external disturbances and to model mismatch. Motivated by these reasons, closed-loop control approaches have been proposed. In [16] the combination of command shaping and feedback control was proposed which can reduce payload oscillation. In [17], a state feedback control law based on linearized model is used to achieve the control objectives. In [18]-[19] the authors proposed a Proportional-Derivative (PD) controller with gravity compensation based on the nonlinear model of the boom crane. In [20] the authors present constrained control for boom cranes.

Most of the existing closed-loop control laws for boom cranes have two main drawbacks:

1. The dynamic of the hoisting mechanism is neglected (e.g. the length of the cable is considered as constant).
2. In the design of the control law, the possibility of measuring the oscillations of the payload (e.g. angular positions and speeds) is usually ignored.

In order to address these problems, we propose a control law that exploits all states of the system to control it. The proposed control scheme is based on a detailed mathematical model in which we take into account all the degrees of freedom (DoFs) that characterize this type of system (i.e. the two rotations, the length of the rope, and

the payload swing angles). Realistic physical parameters of an existing boom crane are used in simulation tests to show the effectiveness of the proposed approach.

## 2 Dynamic Model

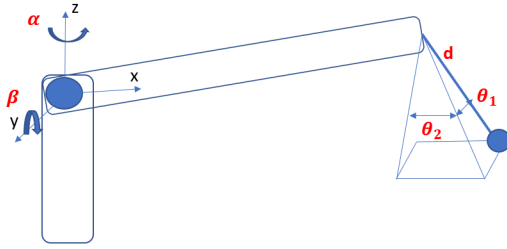


Figure 1. Model of a boom crane

The type of crane considered in this paper (see Fig.1) is represented by five generalized coordinates:  $\alpha$  is the slew angle of the tower,  $\beta$  is the luff angle of the boom,  $d$  is the length of the rope,  $\theta_1$  is the tangential pendulation due to the motion of the tower, and  $\theta_2$  is the radial sway due to the motion of the boom.

The equations of the motion obtained using the Euler-Lagrange approach are

$$\begin{aligned}
 & I_t \ddot{\alpha} + d^2 \ddot{\alpha} m + \ddot{\alpha} l_B^2 m C_\beta^2 + (\ddot{\alpha} l_B^2 m_B C_\beta^2)/4 - d^2 \ddot{\theta}_2 m S_\theta_3 \\
 & + 2d \dot{d} \dot{\alpha} m - 2d^2 \dot{\theta}_1 \dot{\theta}_2 m C_{\theta_1} - d^2 \ddot{\alpha} m C_{\theta_1}^2 C_{\theta_4}^2 - \dot{\alpha} \dot{\beta} l_B^2 m S_{2\beta} \\
 & - (\dot{\alpha} \dot{\beta} l_B^2 m_B S_{2\beta})/4 - 2d \dot{d} \dot{\theta}_2 m S_{\theta_3} + \ddot{d} l_B m C_\beta C_{\theta_4} S_{\theta_3} \\
 & - 2d \dot{d} \dot{\alpha} m C_{\theta_1}^2 C_{\theta_4}^2 + 2d^2 \dot{\theta}_1 \dot{\theta}_2 m C_{\theta_1} C_{\theta_4}^2 + d^2 \dot{\theta}_1 m C_{\theta_1} C_{\theta_4} S_{\theta_4} \\
 & + 2d \ddot{\alpha} l_B m C_\beta S_{\theta_4} + 2d \dot{\alpha} l_B m C_\beta S_{\theta_4} - d^2 \dot{\theta}_1^2 m C_{\theta_4} S_{\theta_3} S_{\theta_4} \\
 & + 2d \dot{\alpha} \dot{\theta}_2 l_B m C_\beta C_{\theta_4} - 2d \dot{\alpha} \dot{\beta} l_B m S_\beta S_{\theta_4} \\
 & + 2d^2 \dot{\alpha} \dot{\theta}_2 m C_{\theta_1}^2 C_{\theta_4} S_{\theta_4} + d \ddot{\theta}_1 l_B m C_\beta C_{\theta_1} C_{\theta_4} \\
 & + 2d \dot{\theta}_1 l_B m C_\beta C_{\theta_1} C_{\theta_4} + 2d \dot{d} \dot{\theta}_1 m C_{\theta_1} C_{\theta_4} S_{\theta_4} \\
 & + d \ddot{\beta} l_B m C_{\theta_4} S_\beta S_{\theta_3} - d \ddot{\theta}_2 l_B m C_\beta S_{\theta_3} S_{\theta_4} \\
 & - 2d \dot{\theta}_2 l_B m C_\beta S_{\theta_3} S_{\theta_4} + d \dot{\beta}^2 l_B m C_\beta C_{\theta_4} S_{\theta_3} \\
 & - d \dot{\theta}_1^2 l_B m C_\beta C_{\theta_4} S_{\theta_3} + 2d^2 \dot{\alpha} \dot{\theta}_1 m C_{\theta_1} C_{\theta_4}^2 S_{\theta_3} \\
 & - d \dot{\theta}_2^2 l_B m C_\beta C_{\theta_4} S_{\theta_3} - 2d \dot{\theta}_1 \dot{\theta}_2 l_B m C_\beta C_{\theta_1} S_{\theta_4} = u_1, \quad (1)
 \end{aligned}$$

$$\begin{aligned}
 & I_B \ddot{\beta} + \dot{\beta} l_B^2 m + (\dot{\beta} l_B^2 m_B)/4 + g l_B m C_\beta + (g l_B m_B C_\beta)/2 \\
 & + (\dot{\alpha}^2 l_B^2 m S_{2\beta})/2 + (\dot{\alpha}^2 l_B^2 m_B S_{2\beta})/8 - \ddot{d} l_B m S_\beta S_{\theta_2} \\
 & - \ddot{d} l_B m C_\beta C_{\theta_1} C_{\theta_2} + d \dot{\alpha}^2 l_B m S_\beta S_{\theta_2} + d \dot{\theta}_2^2 l_B m S_\beta S_{\theta_2} \\
 & - d \dot{\theta}_2 l_B m C_{\theta_2} S_\beta - 2d \dot{\theta}_2 l_B m C_{\theta_2} S_\beta + d \ddot{\theta}_1 l_B m C_\beta C_{\theta_2} S_{\theta_1} \\
 & + d \ddot{\theta}_2 l_B m C_\beta C_{\theta_1} S_{\theta_2} + 2d \dot{\theta}_1 l_B m C_\beta C_{\theta_2} S_{\theta_1} \\
 & + 2d \dot{\theta}_2 l_B m C_\beta C_{\theta_1} S_{\theta_2} + d \dot{\alpha} l_B m C_{\theta_2} S_\beta S_{\theta_1} \\
 & + 2d \dot{\alpha} l_B m C_{\theta_2} S_\beta S_{\theta_1} + d \dot{\theta}_1^2 l_B m C_\beta C_{\theta_1} C_{\theta_2} \\
 & + d \dot{\theta}_2^2 l_B m C_\beta C_{\theta_1} C_{\theta_2} - 2d \dot{\theta}_1 \dot{\theta}_2 l_B m C_\beta S_{\theta_1} S_{\theta_2} \\
 & - 2d \dot{\alpha} \dot{\theta}_2 l_B m S_\beta S_{\theta_1} S_{\theta_2} + 2d \dot{\alpha} \dot{\theta}_1 l_B m C_{\theta_1} C_{\theta_2} S_\beta = u_2, \quad (2)
 \end{aligned}$$

$$\begin{aligned}
 & \ddot{m} - d \dot{\alpha}^2 m - d \dot{\theta}_2^2 m - d \dot{\theta}_1^2 m C_{\theta_2}^2 - g m C_{\theta_1} C_{\theta_2} \\
 & + d \dot{\alpha}^2 m C_{\theta_1}^2 C_{\theta_2}^2 - \dot{\beta} l_B m S_\beta S_{\theta_2} - \dot{\alpha}^2 l_B m C_\beta S_{\theta_2} \\
 & - \dot{\beta}^2 l_B m C_\beta S_{\theta_2} + 2d \dot{\alpha} \dot{\theta}_2 m S_{\theta_1} - \dot{\beta} l_B m C_\beta C_{\theta_1} C_{\theta_2} \\
 & + \dot{\alpha} l_B m C_\beta C_{\theta_2} S_{\theta_1} + \dot{\beta}^2 l_B m C_{\theta_1} C_{\theta_2} S_\beta \\
 & - 2d \dot{\alpha} \dot{\theta}_1 m C_{\theta_1} C_{\theta_2} S_{\theta_2} - 2\dot{\alpha} \dot{\beta} l_B m C_{\theta_2} S_\beta S_{\theta_1} = u_3, \quad (3)
 \end{aligned}$$

$$\begin{aligned}
 & d m C_{\theta_2} (g S_{\theta_1} + 2d \dot{\theta}_1 C_{\theta_2} + d \ddot{\theta}_1 C_{\theta_2} - \dot{\beta}^2 l_B S_\beta S_{\theta_1} \\
 & - 2d \dot{\theta}_1 \dot{\theta}_2 S_{\theta_2} + \dot{\alpha} l_B C_\beta C_{\theta_1} + d \ddot{\alpha} C_{\theta_1} S_{\theta_2} + 2d \dot{\alpha} C_{\theta_1} S_{\theta_2} \\
 & + \dot{\beta} l_B C_\beta S_{\theta_1} - d \dot{\alpha}^2 C_{\theta_1} C_{\theta_2} S_{\theta_1} + 2d \dot{\alpha} \dot{\theta}_2 C_{\theta_1} C_{\theta_2} \\
 & - 2\dot{\alpha} \dot{\beta} l_B C_{\theta_1} S_\beta) = 0, \quad (4)
 \end{aligned}$$

$$\begin{aligned}
 & -d m (d \ddot{\alpha} S_{\theta_1} - 2d \dot{\theta}_2 - d \ddot{\theta}_2 + 2d \dot{\alpha} S_{\theta_1} - g C_{\theta_1} S_{\theta_2} \\
 & - (d \dot{\theta}_1^2 S_{2\theta_2})/2 + \dot{\alpha}^2 l_B C_\beta C_{\theta_2} + \dot{\beta}^2 l_B C_\beta C_{\theta_2} \\
 & + \dot{\beta} l_B C_{\theta_2} S_\beta + \dot{\beta}^2 l_B C_{\theta_1} S_\beta S_{\theta_2} + d \dot{\alpha}^2 C_{\theta_1}^2 C_{\theta_2} S_{\theta_2} \\
 & + 2d \dot{\alpha} \dot{\theta}_1 C_{\theta_1} C_{\theta_2}^2 - \dot{\beta} l_B C_\beta C_{\theta_1} S_{\theta_2} + \dot{\alpha} l_B C_\beta S_{\theta_1} S_{\theta_2} \\
 & - 2\dot{\alpha} \dot{\beta} l_B S_\beta S_{\theta_1} S_{\theta_2}) = 0. \quad (5)
 \end{aligned}$$

where  $m$ ,  $m_b$  denote the load mass, and the boom mass, respectively,  $l_b$  is the boom length,  $I_t$  is the inertia moment of the tower, and  $I_b$  is the inertia moment of the boom. Moreover, the following abbreviations are used:  $S_\alpha \triangleq \sin(\alpha)$ ,  $S_\beta \triangleq \sin(\beta)$ ,  $S_{\theta_1} \triangleq \sin(\theta_1)$ ,  $S_{\theta_2} \triangleq \sin(\theta_2)$ ,  $C_\alpha \triangleq \cos(\alpha)$ ,  $C_\beta \triangleq \cos(\beta)$ ,  $C_{\theta_1} \triangleq \cos(\theta_1)$ ,  $C_{\theta_2} \triangleq \cos(\theta_2)$ .

The system dynamics (1)-(5) can be rewritten in matrix form as

$$M(q) \ddot{q} + C(q, \dot{q}) \dot{q} + G(q) = \begin{bmatrix} I_{3 \times 3} \\ 0_{2 \times 2} \end{bmatrix} u, \quad (6)$$

where  $q = [\alpha, \beta, d, \theta_1, \theta_2]^T \in \mathbb{R}^5$  represents the state vector, and  $u = [u_1, u_2, u_3]^T \in \mathbb{R}^3$  is the control input

vector. The matrices  $M(q) \in \mathbb{R}^{5 \times 5}$ ,  $C(q, \dot{q}) \in \mathbb{R}^{5 \times 5}$ , and  $G(q) \in \mathbb{R}^5$  represent the inertia matrix, centripetal-Coriolis forces, and gravity term, respectively.

As one can see from (6), the boom crane is an under-actuated system, having fewer independent actuators than system degrees of freedom (DoFs). Thus, we can rewrite its model as

$$M_{11}(q)\ddot{q}_1 + M_{12}(q)\ddot{q}_2 + C_{11}(q, \dot{q})\dot{q}_1 + C_{12}(q, \dot{q})\dot{q}_2 + G_1(q) = U, \quad (7)$$

$$M_{21}(q)\ddot{q}_1 + M_{22}(q)\ddot{q}_2 + C_{21}(q, \dot{q})\dot{q}_1 + C_{22}(q, \dot{q})\dot{q}_2 + G_2(q) = 0, \quad (8)$$

where  $q_1 = [\alpha \ \beta \ d]^T$  is the vector of actuated states and  $q_2 = [\theta_1 \ \theta_2]^T$  of non-actuated states and

$$M_{11}(q) = \begin{bmatrix} m_{11} & m_{12} & m_{13} \\ m_{21} & m_{22} & m_{23} \\ m_{31} & m_{32} & m_{33} \end{bmatrix}, M_{12}(q) = \begin{bmatrix} m_{14} & m_{15} \\ m_{24} & m_{25} \end{bmatrix},$$

$$M_{21}(q) = \begin{bmatrix} m_{41} & m_{42} & m_{43} \\ m_{51} & m_{52} & m_{53} \end{bmatrix}, M_{22}(q) = \begin{bmatrix} m_{44} & 0 \\ 0 & m_{55} \end{bmatrix},$$

$$C_{11}(q, \dot{q}) = \begin{bmatrix} c_{11} & c_{12} & c_{13} \\ c_{21} & c_{22} & c_{23} \\ c_{31} & c_{32} & c_{33} \end{bmatrix}, C_{12}(q, \dot{q}) = \begin{bmatrix} c_{14} & c_{15} \\ c_{24} & c_{25} \end{bmatrix},$$

$$C_{21}(q, \dot{q}) = \begin{bmatrix} c_{41} & c_{42} & c_{43} \\ c_{51} & c_{52} & c_{53} \end{bmatrix}, C_{22}(q, \dot{q}) = \begin{bmatrix} c_{44} & 0 \\ 0 & c_{55} \end{bmatrix},$$

$$G_1(q) = \begin{bmatrix} 0 \\ g_2 \\ g_3 \end{bmatrix}, G_2(q) = \begin{bmatrix} g_4 \\ g_5 \end{bmatrix}, U = \begin{bmatrix} u_1 \\ u_2 \\ u_3 \end{bmatrix}.$$

### 3 Control Design

The aim of the control is to move the crane to the desired position and to dampen the swing angles of the load. In our development we will consider the following reasonable assumptions.

**Assumption 1** The payload swing are such that  $|\theta_{1,2}| < \frac{\pi}{2}$ .

**Assumption 2** The cable length is always greater than zero to avoid singularity in the model (6), i.e.  $d(t) > 0, \forall t \geq 0$ .

As one can see, (8) can be rewritten as

$$\ddot{q}_2 = -M_{22}^{-1}(q)(M_{21}(q)\ddot{q}_1 + C_{21}(q, \dot{q})\dot{q}_1 + C_{22}(q, \dot{q})\dot{q}_2 + G_2(q)). \quad (9)$$

It is worth noticing that in (9) the  $M_{22}(q)$  is a positive definite matrix due to Assumptions (1)-(2).

Substituting (9) into (7), one obtains

$$\bar{M}(q)\ddot{q}_1 + \bar{C}_1(q, \dot{q})\dot{q}_1 + \bar{C}_2(q, \dot{q})\dot{q}_2 + \bar{G}(q) = U, \quad (10)$$

where

$$\begin{aligned} \bar{M}(q) &= M_{11}(q) - M_{12}(q)M_{22}^{-1}(q)M_{21}(q), \\ \bar{C}_1(q, \dot{q}) &= C_{11}(q, \dot{q}) - M_{12}(q)M_{22}^{-1}(q)C_{12}(q, \dot{q}), \\ \bar{C}_2(q, \dot{q}) &= C_{12}(q, \dot{q}) - M_{12}(q)M_{22}^{-1}(q)C_{22}(q, \dot{q}), \\ \bar{G}(q) &= G_1(q) - M_{12}(q)M_{22}^{-1}(q)G_2(q). \end{aligned}$$

According to Assumptions (1)-(2), the matrix  $\bar{M}$  is positive definite. Then, (10) can be rewritten as

$$\ddot{q}_1 = \bar{M}^{-1}(q)(U - \bar{C}_1(q, \dot{q})\dot{q}_1 - \bar{C}_2(q, \dot{q})\dot{q}_2 - \bar{G}(q)) \quad (11)$$

Substituting (11) into (9) yields

$$\begin{aligned} \ddot{q}_2 &= -M_{22}^{-1}(q)(M_{21}(q)\bar{M}^{-1}(q)(-\bar{C}_1(q, \dot{q})\dot{q}_1 - \bar{C}_2(q, \dot{q})\dot{q}_2 - \bar{G}(q) + U) \\ &\quad + C_{21}(q, \dot{q})\dot{q}_1 + C_{22}(q, \dot{q})\dot{q}_2 + G_2(q)). \end{aligned} \quad (12)$$

Following the classical approach of a feedback linearization technique, (11) can be “linearized” by using the control law

$$U = \bar{M}(q)v + \bar{C}_1(q, \dot{q})\dot{q}_1 + \bar{C}_2(q, \dot{q})\dot{q}_2 + \bar{G}(q). \quad (13)$$

Thus, (11) becomes

$$\ddot{q}_1 = v, \quad (14)$$

where  $v \in \mathbb{R}^3$  as additional control inputs.

To move the crane to the desired position, the additional control inputs (14) can be chosen as

$$v = \ddot{q}_{1d} - K_{ad}(\dot{q}_1 - \dot{q}_{1d}) - K_{ap}(q_1 + q_{1d}), \quad (15)$$

where  $K_{ad} = \text{diag}(K_{ad1}, K_{ad2}, K_{ad3})$ ,  $K_{ap} = \text{diag}(K_{ap1}, K_{ap2}, K_{ap3})$  are positive diagonal matrices. Substituting (15) into (14), we obtain

$$\ddot{q}_1 + K_{ad}\dot{q}_1 + K_{ap}q_1 = 0, \quad (16)$$

where  $\tilde{q} = q_1 - q_{1d}$  is the tracking error vector of the actuated states. (16) is exponentially stable for every  $K_{ad} > 0$  and  $K_{ap} > 0$ .

To stabilize the non-actuated states  $q_2$ , following what is proposed in [21], we define a second additional inputs as

$$v_u = -K_{ud}\dot{q}_2 - K_{up}q_2, \quad (17)$$

where  $v_u \in \mathbb{R}^2$  are additional inputs which take into account the non-actuated states,  $K_{ad} = \text{diag}(K_{ud1}, K_{ud2})$ ,  $K_{ap} = \text{diag}(K_{up1}, K_{up2})$  are positive diagonal matrices.

Considering  $q_{1d} = \text{const}$ , the overall additional inputs are proposed by linearly combining (15) and (17)

$$v = -K_{ad}\dot{q}_1 - K_{ap}(q_1 - q_{1d}) - \alpha(K_{ud}\dot{q}_2 - K_{up}q_2), \quad (18)$$

where

$$\alpha = \begin{bmatrix} \alpha_1 & 0 \\ 0 & \alpha_2 \\ 0 & 0 \end{bmatrix} \quad (19)$$

is a weighting matrix.

Substituting the (18) into (13) the overall control law is obtained as

$$U = (\bar{C}_1(q, \dot{q}) - \bar{M}(q)K_{ad})\dot{q}_1 + (\bar{C}_2(q, \dot{q}) - \bar{M}(q)\alpha K_{ud})\dot{q}_2 - \bar{M}(q)K_{ap}(q_1 - q_{1d}) - \bar{M}(q)\alpha K_{up}q_2 + \bar{G}(q). \quad (20)$$

Replacing (20) into (12), we obtain

$$\ddot{q}_2 = -M_{22}^{-1}(q)(-M_{21}(q)(K_{ad}\dot{q}_1 + K_{ap}q_1 + \alpha(K_{ud}\dot{q}_2 + K_{up}q_2)) + C_{21}(q, \dot{q})\dot{q}_1 + C_{22}(q, \dot{q})\dot{q}_2 + G_2(q)). \quad (21)$$

Considering Assumption 1, in the rest of this Section we have to demonstrate that (21) converges to the equilibrium point expressed by:  $q_2 = \dot{q}_2 = 0$  to achieve the control goal.

Setting  $q_1 = q_{1d}$  in (21), one achieves

$$\ddot{q}_2 = -M_{22}^{-1}(q)(-M_{21}(q)(\alpha(K_{ud}\dot{q}_2 + K_{up}q_2)) + C_{22}(q, \dot{q})\dot{q}_2 + G_2(q)). \quad (22)$$

The stability analysis of (22) is analyzed by linearizing (22) around the equilibrium point  $q_2 = \dot{q}_2 = 0$ . We can rewrite (22) as

$$z_1 = \theta_1, \quad z_2 = \dot{\theta}_1, \quad z_3 = \theta_2, \quad z_4 = \dot{\theta}_2.$$

Then, we obtain the following state-space forms:

$$\dot{z}_1 = z_2, \quad (23)$$

$$\dot{z}_2 = h_1(z), \quad (24)$$

$$\dot{z}_3 = z_4, \quad (25)$$

$$\dot{z}_4 = h_2(z), \quad (26)$$

with  $z = [z_1 \ z_2 \ z_3 \ z_4]^T$  as a state vector. Linearizing (23)-(26) around  $z = 0$ , we obtain

$$\dot{z} = Az, \quad (27)$$

where

$$A = \begin{bmatrix} 0 & 1 & 0 & 0 \\ \frac{\partial h_1}{\partial z_1} & \frac{\partial h_1}{\partial z_2} & \frac{\partial h_1}{\partial z_3} & \frac{\partial h_1}{\partial z_4} \\ 0 & 0 & 0 & 1 \\ \frac{\partial h_2}{\partial z_1} & \frac{\partial h_2}{\partial z_2} & \frac{\partial h_2}{\partial z_3} & \frac{\partial h_2}{\partial z_4} \end{bmatrix}_{z=0} = \begin{bmatrix} 0 & 1 & 0 & 0 \\ a_{11} & a_{12} & 0 & 0 \\ 0 & 0 & 0 & 1 \\ 0 & 0 & a_{21} & a_{22} \end{bmatrix}. \quad (28)$$

The non-zero elements in (28) are the following:

$$a_{11} = -\frac{(g - a_1 K_{pu1} l_B \cos \beta)}{d}, \quad (29)$$

$$a_{12} = \frac{a_1 K_{du1} l_B \cos \beta}{d}, \quad (30)$$

$$a_{21} = -\frac{(g + a_2 K_{pu2} l_B \sin \beta)}{d}, \quad (31)$$

$$a_{22} = -\frac{a_2 K_{du2} l_B \sin \beta}{d}. \quad (32)$$

The linearized system (27) is stable around the equilibrium point  $z = 0$ , if the A matrix (28) is a Hurwitz matrix. Therefore, it is necessary to properly choose the control parameters that appear in (29)-(32). In this way, (27) is stable around equilibrium point  $z = 0$ , which leads to the local stability of (21). In the Section 4 the values for each of the control parameters are listed.

## 4 Simulation Results

In this section, three different simulation scenarios will be shown to demonstrate the proposed control scheme. In each of them the goal is to move the crane to a desired position and to reduce the swings of the payload as much as possible. In the second and third simulation, the effects of a gust of wind for the payload will be shown.

To get realistic values for the simulation tests, we consider a small boom crane: the NK 1000 Mini Crane from NEMAASKO [22]. Some parameters are taken directly from the datasheets. Others, like the boom dimensions were estimated by CAD simulations.

The crane system parameters are selected as follows:

$$I_t = 207.13 \text{ kgm}^2, \quad l_B = 6.2 \text{ m}, \quad m_B = 312.2 \text{ kg}, \\ I_B = 2068 \text{ kgm}^2, \quad g = 9.81 \text{ ms}^{-2}, \quad m = 50 \text{ kg}.$$

The control parameters for controller (18) are set as  $K_{ad} = \text{diag}(100, 100, 150)$ ,  $K_{ap} = \text{diag}(10, 20, 50)$ ,  $K_{ud} = \text{diag}(120, 120)$ ,  $K_{up} = \text{diag}(10, 10)$ ,  $a_1 = -1$ ,  $a_2 = \text{sign}(\beta)$ .

*Scenario 1.* In this simulation scenario, we show the performance of the proposed control law described in the Section 3. The goal is to move the crane to a desired configuration while damping the payload swing angles as much as possible. In this first scenario no external disturbances to the crane will be considered. The simulation results are shown in Fig.2-6. We can see that the boom arrives at the desired positions in around 30 seconds. Additionally, the maximum payload swing amplitudes in the two directions are confined in  $-2.5^\circ$  and  $1^\circ$ , respectively. In Fig.7 the input controls are shown. For the boom actuator following the [22], the limit of the working range of the crane is of 210kg for the payload mass with a boom length of 8.9m then the maximal torque should be around  $u_{2max} = 18.2 \text{ kNm}$ . The values of the other two inputs do not represent a problem as the inputs values are reasonable and well within the typical limits of the crane actuators.

*Scenario 2.* In this simulation scenario, we consider a gust of wind as external disturbance for the crane. The desired configuration for the crane is the same of the previous scenario. In this case the controller must be able to counteract the effect of wind during the whole movement of the crane. The perturbation seen by the system will be characterized by a duration and a time dependent amplitude. Concerning the first one, a study from a meteorological center of the Netherlands reported that wind gusts have periods of 2 to 7 seconds with average speeds comprised between 4 and 20  $\text{m/s}$  [23]. The force applied on the payload can be seen as distributed force  $F = \frac{1}{2} \rho V^2 A_w C_D$ , where  $V$  is the wind average gust speeds, and  $A_w$  is the surface exposed to the wind. According to [24],  $C_D = 1.05$

will be chosen. Assuming ISA conditions at sea level,  $\rho = 1.225 [\text{kg}/\text{m}^3]$ .

In this Scenario, we consider a force that acts laterally to the load (e.g. increases the swing angle  $\theta_1$ ). In this scenario, only one gust of wind will occur when the simulation is at 20s. In our simulations, the wind speed will have a trapezoidal shape (e.g. increase linearly from zero, constant for a time window and finally linearly decrease to zero).

As one can see in Fig. 11-12, due to the wind gust, the swing angle  $\theta_1$  increases and consequently also the angle  $\theta_2$  oscillates. To counteract this effect, the controller modifies the tower angle  $\alpha$  (Fig.8 and Fig.13) and the boom angle  $\beta$  (Fig.9 and Fig.13) to reduce the swing angles as fast as possible. The small effects on the length of the cable can be seen in Fig.13, where one can see that the force on the cable changes a little.

*Scenario 3.* In this Simulation scenario, the main effect of the wind is on the angle  $\theta_2$ . In this case, the swing radial angle increases (see Fig.18) and consequentially the controller modifies the value of the luff angle (Fig.15) and the length of the cable (Fig.16) to reduce the oscillations as much as possible. There are no significant effects on the angle  $\theta_1$ , therefore no changes are required for the slew angle  $\alpha$ . As one can see in Fig.19, to quickly counteract the effect of the wind, the control input  $u_2$  reaches its limit value and then decreases.

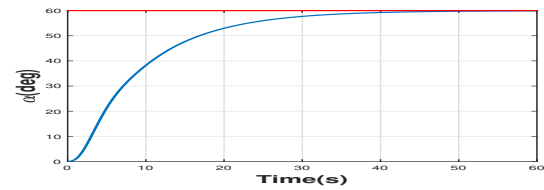


Figure 2. Scenario 1. Tower angle  $\alpha$ . Red line: Desired reference. Blue line: Simulation result.

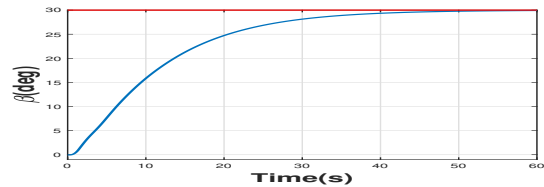


Figure 3. Scenario 1. Boom angle  $\beta$ . Red line: Desired reference. Blue line: Simulation result.

## 5 Conclusion

The paper proposed a detailed mathematical model of a boom crane which takes into account all of the degrees of

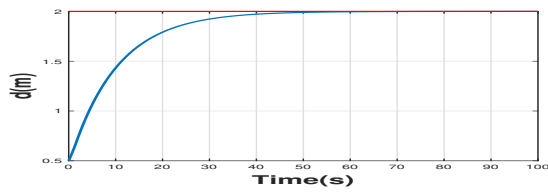


Figure 4. Scenario 1. Cable length. Red line: Desired reference. Blue line: Simulation result.

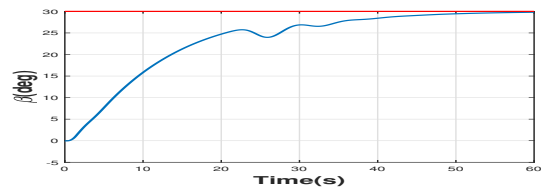


Figure 9. Scenario 2. Boom angle  $\beta$ . Red line: Desired reference. Blue line: Simulation result.

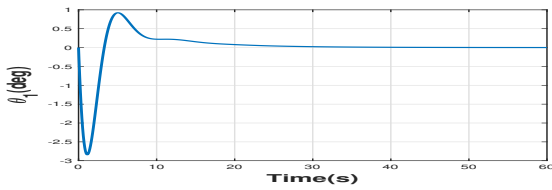


Figure 5. Scenario 1. Payload angle  $\theta_1$ .

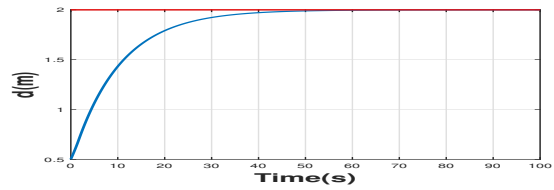


Figure 10. Scenario 2. Cable length. Red line: Desired reference. Blue line: Simulation result.

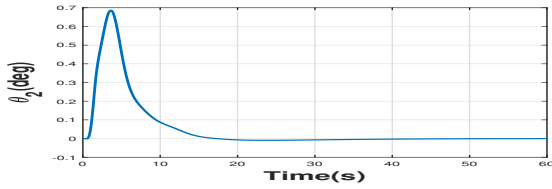


Figure 6. Scenario 1. Payload angle  $\theta_2$ .

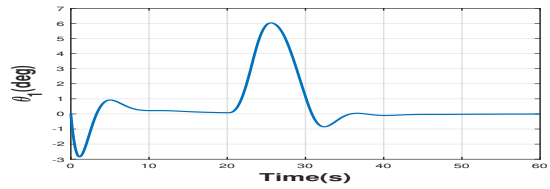


Figure 11. Scenario 2. Payload angle  $\theta_1$ .

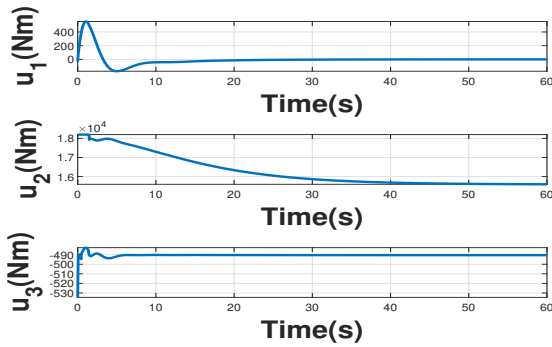


Figure 7. Scenario 1. Control inputs

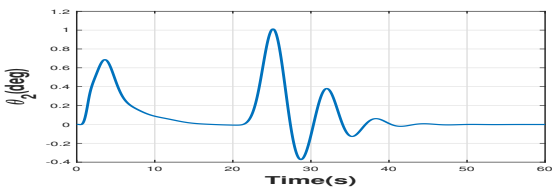


Figure 12. Scenario 2. Payload angle  $\theta_2$ .

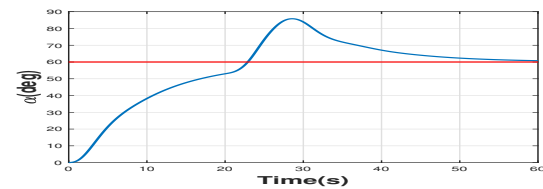


Figure 8. Scenario 2. Tower angle  $\alpha$ . Red line: Desired reference. Blue line: Simulation result.

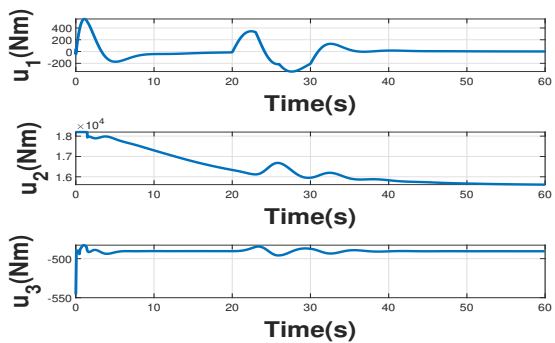


Figure 13. Scenario 2. Control inputs

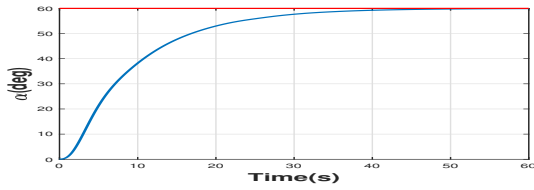


Figure 14. Scenario 3. Tower angle  $\alpha$ . Red line: Desired reference. Blue line: Simulation result.

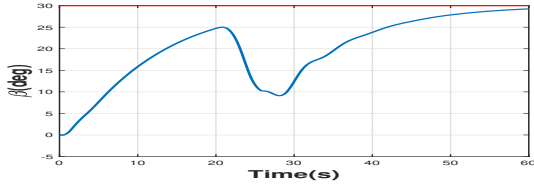


Figure 15. Scenario 3. Boom angle  $\beta$ . Red line: Desired reference. Blue line: Simulation result.

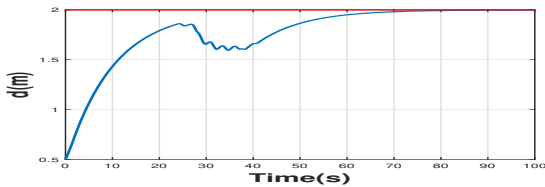


Figure 16. Scenario 3. Cable length. Red line: Desired reference. Blue line: Simulation result.

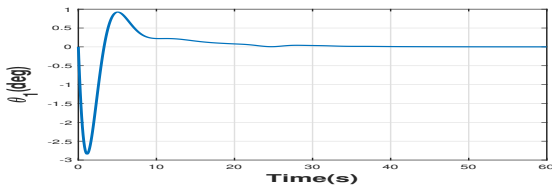


Figure 17. Scenario 3. Payload angle  $\theta_1$ .

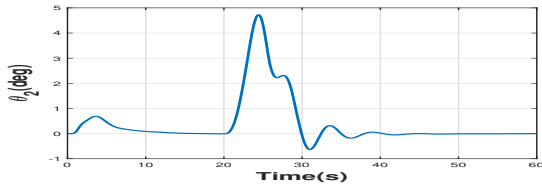


Figure 18. Scenario 3. Payload angle  $\theta_2$ .

freedom (DoFs) that characterize this type of system (i.e. the two rotations, the length of the rope and the payload swing angles). Despite the complexity of the model, we design a nonlinear control law that exploits all the states of the model to guide the crane towards a desired reference

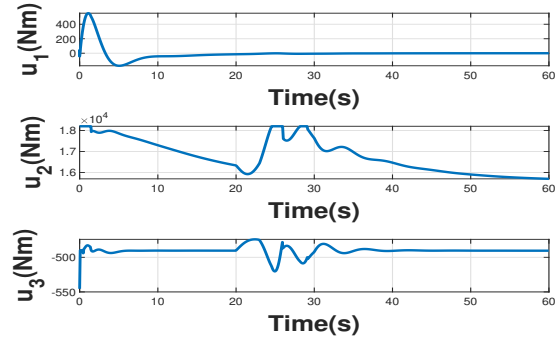


Figure 19. Scenario 3. Control inputs

and ensuring that the non-actuated variables (i.e.,  $\theta_1$  and  $\theta_2$ ) go to zero in a fast way. The simulation results with realistic physical parameters show the efficiency of the proposed control scheme even in the presence of wind disturbance.

## References

- [1] L. A. Tuan, G. Kim, and S. Lee. Partial feedback linearization control of the three dimensional overhead crane. pages 1198–1203, 2012. doi:10.1109/CoASE.2012.6386314.
- [2] N. Sun, Y. Fang, H. Chen, and B. Lu. Amplitude-saturated nonlinear output feedback antiswing control for underactuated cranes with double-pendulum cargo dynamics. *IEEE Transactions on Industrial Electronics*, 64(3):2135–2146, 2017. doi:10.1109/TIE.2016.2623258.
- [3] Le Tuan, Hoang Cuong, Soon-Geul Lee, Nho Cong, and Kee Moon. Nonlinear feedback control of container crane mounted on elastic foundation with the flexibility of suspended cable. *Journal of Vibration and Control*, 22, 11 2014. doi:10.1177/1077546314558499.
- [4] Ning Sun, Yongchun Fang, He Chen, Yiming Wu, and Biao lu. Nonlinear antiswing control of offshore cranes with unknown parameters and persistent ship-induced perturbations: Theoretical design and hardware experiments. *IEEE Transactions on Industrial Electronics*, PP:1–1, 10 2017. doi:10.1109/TIE.2017.2767523.
- [5] Naoki Uchiyama, Huimin Ouyang, and Shigenori Sano. Simple rotary crane dynamics modeling and open-loop control for residual load sway suppression by only horizontal boom motion. *Mechatronics*, 23:1223–1236, 12 2013. doi:10.1016/j.mechatronics.2013.09.001.

- [6] M. Ambrosino, B. Thierens, A. Dawans, and E. Garone. Oscillation reduction for knuckle cranes. In *ISARC. Proceedings of the International Symposium on Automation and Robotics in Construction*, 2020.
- [7] Zhiyu Xi and Tim Hesketh. Discrete time integral sliding mode control for overhead crane with uncertainties. *Control Theory & Applications, IET*, 4:2071 – 2081, 11 2010. doi:10.1049/iet-cta.2009.0558.
- [8] Raja Mohd Taufika Raja Ismail and Quang Ha. Trajectory tracking and anti-sway control of three-dimensional offshore boom cranes using second-order sliding modes. pages 996–1001, 08 2013. doi:10.1109/CoASE.2013.6654071.
- [9] Aurelio Piazzzi and Antonio Visioli. Optimal dynamic-inversion-based control of an overhead crane. *Control Theory and Applications, IEE Proceedings -*, 149:405 – 411, 10 2002. doi:10.1049/ip-cta:20020587.
- [10] Ning Sun, Yiming Wu, Yongchun Fang, and He Chen. Nonlinear antiswing control for crane systems with double-pendulum swing effects and uncertain parameters: Design and experiments. *IEEE Transactions on Automation Science and Engineering*, PP:1–10, 07 2017. doi:10.1109/TASE.2017.2723539.
- [11] Eckhard Arnold, Oliver Sawodny, J. Neupert, and Klaus Schneider. Anti-sway system for boom cranes based on a model predictive control approach. *IEEE International Conference Mechatronics and Automation, 2005*, 3:1533–1538 Vol. 3, 2005.
- [12] Kunihiko Nakazono, Kouhei Ohnishi, Hiroshi Kinjo, and Tetsuhiko Yamamoto. Vibration control of load for rotary crane system using neural network with ga-based training. *Artificial Life and Robotics*, 13 (1):98–101, Dec 2008.
- [13] N. Uchiyama, H. Ouyang, and S. Sano. Residual load sway suppression for rotary cranes using only s-curve boom horizontal motion. pages 6258–6263, 2012. doi:10.1109/ACC.2012.6315369.
- [14] Shigenori Sano, Huimin Ouyang, and Naoki Uchiyama. Residual load sway suppression for rotary cranes using simple dynamics model and s-curve trajectory. *IEEE International Conference on Emerging Technologies and Factory Automation, ETFA*, 12818107128151203528138151281510123126851333674122135: 1–5, 09 2012. doi:10.1109/ETFA.2012.6489665.
- [15] Reza Ezuan Samin, Zaharuddin Mohamed, Jamaludin Jalani, and Rozaimi Ghazali. Input shaping techniques for anti-sway control of a 3-dof rotary crane system. *Proceedings - 1st International Conference on Artificial Intelligence, Modelling and Simulation, AIMS 2013*, pages 184–189, 11 2014. doi:10.1109/AIMS.2013.36.
- [16] Jie Huang, Ehsan Maleki, and W.E. Singhose. Dynamics and swing control of mobile boom cranes subject to wind disturbances. *Control Theory & Applications, IET*, 7:1187–1195, 06 2013. doi:10.1049/iet-cta.2012.0957.
- [17] R. Kondo and S. Shimahara. Anti-sway control of a rotary crane via switching feedback control. 1:748 – 752 Vol.1, 10 2004. doi:10.1109/CCA.2004.1387303.
- [18] Tong Yang, Ning Sun, Yuzhe Qian, and Yongchun Fang. An antiswing positioning controller for rotary cranes. pages 1586–1590, 07 2017. doi:10.1109/CYBER.2017.8446568.
- [19] Ning Sun, Tong Yang, Yongchun Fang, Biao lu, and Yuzhe Qian. Nonlinear motion control of underactuated 3-dimensional boom cranes with hardware experiments. *IEEE Transactions on Industrial Informatics*, PP:1–1, 09 2017. doi:10.1109/TII.2017.2754540.
- [20] M. Ambrosino, A. Dawans, and E. Garone. Constraint control of a boom crane system. In *ISARC. Proceedings of the International Symposium on Automation and Robotics in Construction*, 2020.
- [21] L. A. Tuan, G. Kim, and S. Lee. Partial feedback linearization control of the three dimensional overhead crane. pages 1198–1203, 2012. ISSN 2161-8089. doi:10.1109/CoASE.2012.6386314.
- [22] NEBOMAT. *NK 1000 User Manual*. NEBOMAT, 2005.
- [23] F. J. Verheij, J. W. Cleijne, and J. A. Leene. Gust modelling for wind loading. *Journal of Wind Engineering and Industrial Aerodynamics*, 42:947–958, October 1992. ISSN 0167-6105. URL <http://www.sciencedirect.com/science/article/pii/016761059290101F>.
- [24] Liebherr. *Wind influence on crane operations*, 2017. 4th Edition.